HHS Public Access

Author manuscript

Cell Rep. Author manuscript; available in PMC 2018 December 11.

Published in final edited form as:

Cell Rep. 2018 August 07; 24(6): 1484–1495. doi:10.1016/j.celrep.2018.07.010.

p53 Regulates the Expression of LRP1 and Apoptosis through a Stress Intensity-Dependent MicroRNA Feedback Loop

Patrick L. Leslie[1,2], **Derek A. Franklin**[1,3], **Yong Liu**[1,4], and **Yanping Zhang**[1,3,4,5,*]

[1]Department of Radiation Oncology and Lineberger Comprehensive Cancer Center, University of North Carolina at Chapel Hill, Chapel Hill, NC 27599-7461, USA

[2]Curriculum in Genetics and Molecular Biology, University of North Carolina at Chapel Hill, Chapel Hill, NC 27599-7461, USA

[3]Department of Pharmacology, School of Medicine, University of North Carolina at Chapel Hill, Chapel Hill, NC 27599-7461, USA

[4]Jiangsu Center for the Collaboration and Innovation of Cancer Biotherapy, Cancer Institute, Xuzhou Medical College, Xuzhou, Jiangsu 221002, China

[5]Lead Contact

SUMMARY

Understanding how p53 activates certain gene programs and not others is critical. Here, we identify *low-density lipoprotein receptor-related protein 1* (*LRP1*), a transmembrane endocytic receptor, as a p53 target gene. We show that, although *LRP1* transcript expression is upregulated in response to both sub-lethal and lethal doses of p53-activating stress, LRP1 protein is only upregulated in response to sub-lethal stress. Interestingly, lethal doses of p53-activating stress inhibit LRP1 *de novo* translation through an miRNA-based translational repression mechanism. We show that the p53-regulated miRNAs miR-103 and miR-107 are significantly upregulated by lethal doses of stress, resulting in suppression of LRP1 translation and cell death. Our results define a negative feedback loop involving the p53-regulated coding gene *LRP1* and p53-regulated miRNA genes. These findings provide mechanistic insight into the selective expression of p53 target genes in response to different stress intensities to elicit either cell survival or cell death.

In Brief

Leslie et al. uncover a p53-dependent feedback loop whereby p53-regulated protein-coding genes are inhibited by p53-regulated microRNAs in a stress intensity-dependent manner, resulting in

*Correspondence: ypzhang@med.unc.edu.

AUTHOR CONTRIBUTIONS

Conceptualization, P.L.L. and Y.Z.; Methodology, P.L.L., Y.L., and Y.Z.; Validation, P.L.L. and D.A.F.; Investigation, P.L.L., Y.L., and D.A.F.; Resources, Y.Z.; Writing – Original Draft, P.L.L.; Writing – Review & Editing, P.L.L., D.A.F., Y.L., and Y.Z.; Visualization, P.L.L. and Y.Z.; Supervision, Y.Z.; Funding Acquisition, Y.Z. and P.L.L.

DECLARATION OF INTERESTS

The authors declare no competing interests.

SUPPLEMENTAL INFORMATION

Supplemental Information includes six figures and can be found with this article online at https://doi.org/10.1016/j.celrep.2018.07.010.

increased cell death. The findings provide insight into how p53 controls the expression of its target genes to induce a pro-survival or pro-death response to stress.

Graphical Abstract

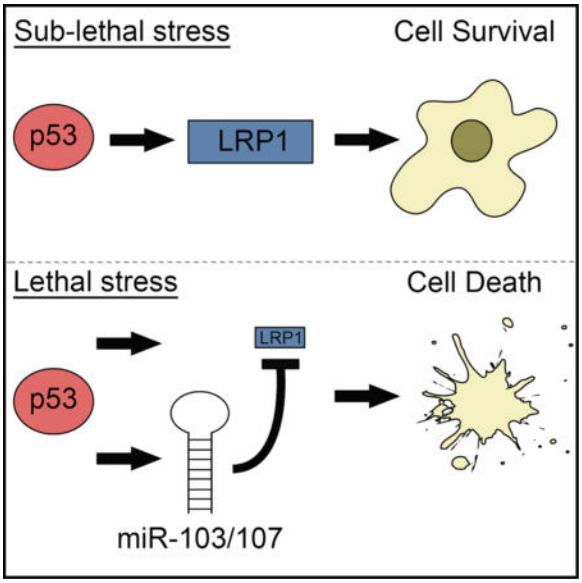

INTRODUCTION

The tumor suppressor p53 is a transcription factor that regulates a diverse set of genes and contributes to the regulation of numerous pathways. Some of the classical functions of p53 include induction of cell cycle arrest and apoptosis, whereas more recently characterized functions of p53 include induction of metabolic alterations, DNA damage repair, and antioxidant responses. As the regulatory functions of p53 increase in scope, the functions of p53 can be broadly categorized into a pro-death and pro-survival dichotomy that is highly context-dependent (Purvis et al., 2012). Thus, although previous studies have explored p53 signaling in either a pro-survival or a pro-apoptotic context, the effect of p53 activation depends on multiple factors, including cell type and the stressors to which the cell is exposed (Kruiswijk et al., 2015). For example, p53 predominantly activates pro-survival genes in response to low concentrations of DNA-damaging agents but predominantly activates proapoptotic genes in response to high concentrations of DNA-damaging agents (Paek et al., 2016). These observations suggest that p53 serves as a decision node for cells under stress that must weigh all inputs, such as the extent of DNA damage and oxidation, and commit the cell to repair the damage or apoptose if the damage is irreparable. Some of the mechanisms involved in this selective p53 gene regulation include post-translational modification of p53 (Rinaldo et al., 2007), p53 protein induction levels (Kracikova et al., 2013), differences in promoter binding affinity (Szak et al., 2001; Weinberg et al., 2005), p53 induction dynamics (Purvis et al., 2012), and co-factor recruitment (Koutsodontis et al., 2005).

The importance of p53 in the decision between the life and death of the cell helps explain why p53 signaling is almost universally perturbed in cancers by direct mutations or by

mutations to proteins that regulate p53 (Leslie and Zhang, 2016). p53 is the most commonly mutated gene in cancer, which has contributed to its popularity as a research topic (Hollstein et al., 1991). However, despite the abundance of p53 publications and its frequent mutation in cancer, we have yet to generate a clinically proven tool for the imaging, prognostication, or treatment of patient cancers based on p53. Although several targeted p53-activating drugs are in clinical development, the possibility exists that these drugs will be either ineffective or counter-productive because p53 is expressed in normal cells as well. Although the general reactivation of p53 is sufficiently selective to target tumor cells while sparing normal cells in mice, whether this holds true for humans remains uncertain (Martins et al., 2006; Ventura et al., 2007; Xue et al., 2007). Indeed, on-target toxicity is a common reason why p53-activating therapies fail. Moreover, p53 activation in cancer cells could generate a pro-survival effect in response to chemotherapies by allowing the cell a chance to repair DNA damage (Chang et al., 1999; Jackson et al., 2012), and this pro-survival role of wild-type (WT) p53 could also be true in human tumors (Bertheau et al., 2013).

One of the barriers to developing clinically useful therapies is our incomplete understanding of the p53 regulome. Understanding not only which genes are regulated by p53 but also in which contexts they are regulated is important to grasp a comprehensive picture of the effects of p53 activation under different conditions. p53 transcriptionally regulates several microRNA genes that could regulate hundreds, if not thousands, of other genes (Hermeking, 2012). However, whether p53-regulated micro-RNAs (miRNAs) affect the expression of p53 target genes remains undetermined. In this study, we begin by identifying the p53 target gene *low-density lipoprotein receptor-related protein 1* (*LRP1*), a multi-functional transmembrane protein involved in endocytosis and signal transduction. Interestingly, we show that p53 regulates LRP1 through a stress intensity-dependent miRNA feedback loop involving the p53-regulated miRNAs miR-103 and miR-107. Importantly, LRP1 suppression is sufficient to induce cell death in cancer cells, suggesting that p53-mediated suppression of LRP1 in response to lethal stress contributes to a pro-death response. Our results describe a p53-driven switch from cell survival to apoptosis whereby p53 inhibits the expression of its own target protein-coding genes through an miRNA-based mechanism. Moreover, based on the connections between LRP1 and several diseases for which the etiology is not completely understood, including cancer, Alzheimer's disease, and atherosclerosis, the identification of LRP1 regulation by p53 in a stress intensity-dependent manner represents an important advancement in several research fields.

RESULTS

p53 Induces LRP1 Expression through Direct Promoter Binding

To identify p53 target genes, we mined a microarray screen previously reported by our lab (Deisenroth et al., 2011; Franklin et al., 2016). In this microarray screen, we compared the expression profiles of three different mouse embryonic fibroblast (MEF) genotypes that express p53 at low (*Mdm2*$^{+/+}$), medium (*Mdm2*$^{-/-}$), or high (*Mdm2*$^{462/462}$) levels (Deisenroth et al., 2011). One of the target genes we identified through this screen was *LRP1*, which closely mirrored the expression pattern of the p53 target gene *Cdkn1a* (*p21*; Figure 1A). Importantly, p53-dependent expression is not observed for the related genes

low-density lipoprotein receptor (*Ldlr*) or *LRP2* (Figure 1A). LRP1 is a transmembrane endocytic receptor that is closely associated with several diseases that remain poorly understood, including Alzheimer's disease, atherosclerosis, and cancer (Gonias and Campana, 2014). To confirm that LRP1 is expressed in a p53-dependent manner, we compared HCT116 colon cancer cells in which we deleted p53 by CRISPR/Cas9 using small guide RNAs targeting *p53* exons 3 (p53 knockout-3 [p53KO-3]) or 5 (p53KO-5). Compared with the control KO line (Ctrl), deletion of p53 reduced basal LRP1 transcript and protein expression to barely detectable levels and abrogated the effect of nutlin-3a treatment on LRP1 induction (Figures 1B and 1C). To show that p53 is sufficient to upregulate LRP1 expression, we transfected p53-null H1299 cells with WT or mutant p53 (R273H), treated these cells with nutlin-3a, and then analyzed LRP1 protein expression. Consistent with a role in LRP1 induction, WT p53 transfection induced LRP1 protein expression and showed a further nutlin-3a-dependent increase in expression (Figure 1D). LRP1 expression was unchanged in empty vector-transfected cells regardless of nutlin-3a treatment. Interestingly, the p53R273H mutant could induce LRP1 protein expression above background levels and showed a nutlin-3a response, suggesting that this p53 mutant retains some ability to transactivate LRP1 expression (but not p21 expression) when overexpressed.

Next we investigated whether LRP1 is a direct p53 target. Analyzing the upstream promoter region of the LRP1 genomic locus revealed one putative p53 response element (RE) that displayed extensive similarity with the consensus RE sequence $(RRRCYYGWWW)_2$ (Wang et al., 2009; Figure 1E). We tested whether this putative p53 RE could be bound by p53 by chromatin immunoprecipitation (ChIP)-qPCR analysis. As predicted, the putative p53 RE was immunoprecipitated in a p53-dependent manner. Moreover, this binding was enhanced by nutlin-3a treatment (Figure 1F). Cloning the putative *LRP1* p53 RE upstream of a luciferase reporter construct was also sufficient to drive luciferase expression in a p53-dependent manner, suggesting that the LRP1 promoter contains a *bona fide* p53 RE that exhibits similar activity relative to the WT p21 p53 RE (Figure 1G). Importantly, mutation of the conserved C and G nucleotides within the putative LRP1 p53 RE abolished the ability of this promoter to drive luciferase expression (Figure 1G).

LRP1 Is Induced by p53-Activating Stresses

Next we tested p53-activating stimuli to determine which stresses upregulate LRP1. For this experiment, we tested the physical DNA damage inducers ionizing radiation and UV-C irradiation, the topoisomerase inhibitors doxorubicin and etoposide, the ribosomal stress inducers low-concentration actinomycin D (ActD) and 5-fluorouracil (5FU), and the DNA adduct-inducing agent cisplatin. Nutlin-3a treatment was used as a positive control. Although all of these stresses were able to induce p53, LRP1 protein induction varied considerably depending on the type of stress (Figure 2A). The highest levels of LRP1 induction occurred in response to the double-strand break-inducing stresses (ionizing radiation [IR], doxorubicin, and etoposide). Moreover, p53 protein stabilization was not necessarily indicative of LRP1 induction because strong p53 induction was observed in response to ActD and 5FU, but only modest LRP1 induction was observed. LRP1 expression appears to depend on p53 in HCT116 cells in response to acute stress because p53 KO HCT116 cells (p53KO-5) showed no detectable induction of LRP1 expression in response to

any of the stresses tested (Figure 2A). LRP1 transcript expression levels were consistent with protein expression levels (Figure 2B). These results are not cell-type-specific because they could be reproduced in the p53 WT osteosarcoma cell line U2OS (Figure S1).

Sub-lethal but Not Lethal Stresses Induce LRP1 Expression

Based on our panel of p53-activating stresses (Figure 2A), we noted a rough correlation whereby stresses that induce extensive cell death, as observed by microscopy (UV irradiation and cisplatin), fail to induce LRP1. We also observed that, although 200 nM doxorubicin induced LRP1 protein, a higher dose of 1 μM doxorubicin failed to induce LRP1 protein despite strong p53 induction (Figure 3A). To gain insight into the periodic administration of chemotherapies typical of patient treatment schedules, we also tested the ability of a brief exposure of 1 μM doxorubicin (sub-lethal doxorubicin or doxorubicin [Dox] pulse) to induce LRP1 compared with 1 μM constant exposure (lethal Dox or Dox hi). Interestingly, 1 hr of 1 μM Dox treatment also strongly induced LRP1 expression (Figure 3A). Moreover, the induction of LRP1 in response to all of the treatments we tested correlated with the cellular outcome, whereby treatments that resulted in cell survival induced LRP1 protein expression, and treatments that resulted in cell death failed to induce LRP1 protein expression. Therefore, we further investigated whether this correlation was also true on the molecular level. We compared the expression of LRP1 and cell death markers in multiple sub-lethal-lethal pairs of stresses (IR versus UV irradiation, Dox pulse versus Dox hi, and etoposide [Etop] low versus Etop high). Propidium iodide-based cell cycle analysis of these treatment pairs revealed the expected large percentage of cells in sub-G1 for UV irradiation, Dox hi, and Etop high at the 24- and 48-hr time points; cell death was noticeably lower in samples treated with the corresponding sub-lethal stresses (Figure 3B). Analysis of protein lysates from the same experiment demonstrated a strong inverse correlation between the induction of LRP1 protein and the expression of apoptotic markers cleaved caspase-3 and cleaved PARP at 24 and 48 hr (Figure 3C). To rule out the possibility that lethal stresses kill the cells too quickly for LRP1 expression to occur, we repeated the experiment using the caspase inhibitor 5-(2,6-Difluorophenoxy)-3-[[3-methyl-1-oxo-2-[(2-quinolinylcarbonyl) amino]butyl]amino]-4-oxo-pentanoic acid hydrate (QVD). Although QVD treatment effectively prevented cell death, as determined by inhibition of caspase-3 cleavage, QVD treatment was insufficient to allow cells to express LRP1 in the presence of lethal stress (Figure 3D), implying a mechanism through which LRP1 protein expression is suppressed.

To further investigate the induction of LRP1, we more closely analyzed the effects of sub-lethal and lethal Dox treatment on DNA damage and DNA damage repair. As expected, comet assay data revealed that Dox pulse allows DNA damage to be repaired whereas Dox hi does not (Figures S2A and S2B). Next we conducted a detailed time course experiment to determine whether LRP1 is induced transiently between 1 and 24 hr after treatment and how p53 levels compare with LRP1 induction. Interestingly, although p53 is induced with similar kinetics in cells treated with lethal Dox compared with sub-lethal Dox, only sub-lethal Dox treatment is able to induce LRP1 protein, and induction occurs between 12 and 24 hr after treatment (Figures 4A–4C). This pattern was also observed when comparing IR and UV-C treatment (Figure S3). These observations are not cell-type-specific because similar trends

were observed in the breast cancer cell line MCF-7 for sub-lethal and lethal Dox (Figures S4A–S4C) as well as IR and UV irradiation (Figures S4D–S4F). To determine the range of doses that correspond to LRP1 induction, we tested the ability of several different doses of Dox to induce LRP1 after a 24-hr treatment period. We found that doses from as low as 50 nM to as high as 900 nM showed clear increases in LRP1 protein expression at 24 hr. The highest concentration of Dox (1,000 nM) did not appreciably induce LRP1 protein expression (Figure 4D). Interestingly, we found a dose-dependent increase, peak, and decrease in LRP1 expression (Figure 4D). Similar results were observed in cells treated with increasing doses of Etop (Figure 4E). Because the β subunit of LRP1 is membrane-embedded and subjected to cleavage by cellular proteases, including beta- and gamma-secretase (Lleó et al., 2005; May et al., 2002; von Arnim et al., 2005), we tested whether the decrease in full-length LRP1 β-subunit protein could be due to LRP1 cleavage. Using a polyclonal LRP1 antibody, we were unable to detect any LRP1 cleavage products by western blot, suggesting that other mechanisms of LRP1 protein repression are responsible for our observation (Figure S5). Because p53 regulates the expression of several pro-apoptotic genes as well, we analyzed the effect of increasing the dose of Dox on the expression levels of Apaf1, Puma, and Noxa. Interestingly, and consistent with the pro-death phenotype observed at high doses of Dox, the pro-apoptotic protein Apaf1 showed considerably higher expression upon treatment with lethal Dox compared with sub-lethal Dox at 24 and 48 hr (Figure 4F). Likewise, the transcript expression levels of Apaf1, Noxa, and Puma showed significant increases upon treatment with lethal Dox compared with sub-lethal Dox (Figure 4G). Altogether, our data indicate that LRP1 protein induction is highly dependent on the intensity of the stress.

Lethal Doses of Dox Result in Suppression of LRP1 Translation

Next we analyzed the transcript levels of *LRP1* and *p21* in response to 50, 200, or 1,000 nM constant Dox treatment or 1 hr pulsed Dox treatment. Interestingly, although we observed low protein expression levels for LRP1 in response to high Dox compared with low Dox, we saw a dose-dependent increase in *LRP1* transcript expression (Figure 5A). p53 ChIP-qPCR analysis also revealed increased p53 binding at the *LRP1* promoter for all Dox treatments (Figure 5B). These results collectively suggest that p53-mediated *LRP1* transcript expression remains increased in the presence of all concentrations of Dox despite the observed low levels of LRP1 protein induction at lethal doses of Dox. Moreover, in the context of our analysis of pro-apoptotic p53 target genes, our results suggest selective suppression of some p53 coding genes (LRP1; Figures 4A–4D) but not others (APAF1, NOXA, or PUMA) (Figures 4F and 4G).

Based on the observed decrease in LRP1 protein in response to lethal stress, we considered two possible explanations: decreased LRP1 protein stability and active translational suppression through miRNAs. To assess the possibility of LRP1 protein degradation, we attempted to determine which protein degradation pathway might account for the difference in LRP1 stability. LRP1 has been reported to undergo insulin-induced degradation that can be inhibited by the proteasome inhibitor MG132 (Ceschin et al., 2009); therefore, we tested whether MG132-mediated proteasome inhibition could rescue LRP1 protein expression in the presence of lethal Dox. Consistent with previous reports, we observed a slight MG132-

dependent increase in LRP1 protein expression at basal levels (Figure 5C, lane 2); however, the extent of the MG132-induced increase in LRP1 protein was notably less than the Dox-induced increase in LRP1. Moreover, MG132 was unable to increase LRP1 protein expression in response to lethal or sub-lethal stress. Unexpectedly, we observed a paradoxical decrease in LRP1 protein upon MG132 treatment for Dox pulse and Dox hi (Figure 5C, lanes 5 and 8). Because LRP1 is associated with the endosome-lysosome pathway, we also attempted to rescue LRP1 protein expression using the lysosome inhibitor chloroquine (CQ), but CQ was unable to rescue LRP1 expression (Figure 5C). These results suggest that the decrease in LRP1 protein expression in response to lethal Dox is not due to increased degradation via the proteasome or lysosome.

To assess the possibility of post-transcriptional regulation of LRP1, we conducted a ^{35}Cys/^{35}Met pulse labeling experiment, which revealed that *de novo* translation of LRP1 is reduced in the presence of lethal Dox compared with sub-lethal Dox, suggesting that Dox dose-dependent regulation of LRP1 protein levels occurs through inhibition of translation (Figure 5D).

Lethal Dox Induces the p53-Regulated miRNAs MiR-103 and MiR-107 to Suppress LRP1 Translation

Because translation inhibition likely occurs through an miRNA-dependent mechanism, we performed a TargetScan search of the LRP1 3′ UTR, and we identified three potential miRNA binding sites corresponding to miR-205, miR-200b/c, and miR-103/ 107 (Figure S6A). Interestingly, all of these miRNA species can be regulated by one or more members of the p53 family (p53, p63, and p73) (Chang et al., 2007; Piovan et al., 2012). Using TaqMan miRNA assays to analyze the expression levels of these miRNAs, we only observed significant Dox dose- and time-dependent increases in the expression levels of miR-103 and miR-107 (Figures 6B and 6C; Figure S6B). We also observed dose-dependent increases in miR-103 and miR-107 expression levels upon treatment with the p53-activating agents Etop, ActD, and cisplatin (Figure S7). Using our CRISPR p53KO HCT116 cell lines, we found p53-dependent induction of these miRNAs upon nutlin-3a treatment (Figure 6A). Next we used a luciferase reporter construct in which the WT 3′ UTR of human *LRP1* was fused downstream of luciferase. Then we tested the ability of the exogenously administered miRNAs miR-103 and miR-107 to suppress the expression of this luciferase construct. Consistent with direct inhibition of luciferase expression through the predicted seed region, the luciferase signal was reduced significantly in the presence of miR-103 and miR-107 (Figure 6D). Moreover, when the predicted miR-103/107 seed region was mutated, luciferase signal inhibition was abrogated, suggesting that this seed region is a bona fide miRNA regulation site in *LRP1* (Figure 6D). To determine whether miR-103/107 regulate endogenous LRP1 protein, we co-transfected miR-103 and 107 mimics or antagomirs into HCT116 cells and then analyzed protein expression levels. Consistent with regulation of LRP1, we observed decreased LRP1 protein expression in response to miR-103/107 mimics and increased expression in response to miR-103/107 antagomirs (Figure 6E). Importantly, LRP1 knockdown is sufficient to induce considerable cell death and G2 arrest in unstimulated HCT116 cells, which corresponds with a dramatic upregulation of cleaved caspase-3 (Figures 6F–6H). Finally, treatment of HCT116 cells with miR-103/107

antagomirs significantly rescued cells from lethal Dox-induced cell death (Figure 6I), suggesting that miR-103- and miR-107-dependent suppression of LRP1 contributes to the pro-death process in HCT116 cells. Collectively, these results suggest that p53 actively suppresses LRP1 protein expression in response to lethal doses of stress by upregulating the miRNAs miR-103 and miR-107 to promote cell death in HCT116 cells.

DISCUSSION

As studies continue to expand our knowledge of the p53 regulome, we present evidence confirming *LRP1* as a direct p53 target gene. Strikingly, deletion of the *TP53* gene in HCT116 cells reduces LRP1 expression to barely detectable levels, suggesting that, at least in colorectal cancer cells, p53 is necessary for LRP1 expression under basal conditions and in response to stress. Interestingly, although *LRP1* transcript levels remain elevated in response to both sub-lethal and lethal stress, LRP1 protein expression is only upregulated in the presence of sub-lethal stress. In the presence of lethal stress, LRP1 protein expression is actively suppressed at the post-transcriptional level, whereas the expression levels of several p53-regulated pro-apoptotic target genes remain elevated. Interestingly, treatment with inhibitors of miR-103 and miR-107 demonstrated significant rescue of LRP1 protein expression and of Dox-induced cell death. Collectively, our results support a mechanism of active inhibition of *de novo* LRP1 translation through a p53-dependent miRNA regulatory feedback mechanism involving miR-103 and miR-107, although we cannot rule out the participation of other miRNAs (Figure 6J). We hypothesize that the active suppression of genes in response to lethal doses of stress could be necessary to efficiently induce the cell death response.

Of interest for future studies is to determine how many and which types of p53-regulated genes could be affected by this mode of feedback regulation. Because the panoply of p53 target genes includes those that could be counter-productive to rapid induction of apoptosis, our results suggest that p53 has a built-in mechanism that allows active suppression of cell survival-type p53 target genes under acutely lethal conditions. Several p53 target genes have been reported to exert anti-apoptotic effects. For example, p21 deletion predisposes cells to initiate an apoptotic p53 response, suggesting that p21 could play a role in preventing apoptosis (Mahyar-Roemer and Roemer, 2001; Waldman et al., 1996). Several mechanisms have been proposed to explain how p21 prevents apoptosis, including procaspase-3 inhibition (Suzuki et al., 1998), inhibition of pro-apoptotic cyclin-dependent kinases (CDKs) (Sohn et al., 2006), and inhibition of apoptosis signal-regulating kinase 1 (Huang et al., 2003). Thus, in response to acute apoptotic stress, it seems likely that inhibition of cell survival genes, such as *p21*, is necessary to rapidly induce apoptosis. LRP1 suppression has similarly been reported to sensitize cells to stress-induced cell death (Campana et al., 2006; Fuentealba et al., 2009; Hamlin et al., 2016). Our results presented here also show that not only is LRP1 suppression sufficient to induce cell death in colorectal cancer cells, but its suppression at the endogenous level appears to occur through a p53-regulated self-switch from pro-survival to pro-apoptosis. Other p53-regulated cell survival and adaptation pathways, including lipid and glucose metabolism, antioxidant pathways, and DNA damage repair, are also likely counterproductive with respect to cell resource allocation in the presence of acute apoptotic stresses.

Interestingly, p53-regulated miRNAs have been reported to silence p53 target genes in separate studies. In one example, the p53-regulated miRNA miR-23a (Yamakuchi et al., 2010) targets the pro-apoptotic p53 target gene *APAF1* (Chen et al., 2014). These results suggest that p53 may also suppress the expression of its pro-apoptotic target genes in certain contexts. In future studies, it would be interesting to determine whether p53 may suppress the expression of its own pro-apoptotic target genes under sub-lethal stress conditions through the upregulation of other miRNAs.

Our results also have interesting clinical implications for the use of double-stranded DNA (dsDNA) break-inducing chemotherapies in the treatment of cancer. Dox has become a staple for the treatment of several solid tumors, including cancers of the uterus, cervix, prostate, pancreas, liver, and connective tissue. Therefore, our finding that sub-lethal doses of Dox could actually promote a p53-dependent cell survival and adaptation response suggests that sub-optimal doses of Dox could induce cancer cell survival in three-dimensional tumors. Because tumors are often poorly perfused in sometimes large areas, it is conceivable that intravenous drugs such as Dox might not accumulate at a high enough concentration in hypoperfused portions of the tumor, which could result in induction of a distinct set of genes that promote cell survival and tumor cell longevity (Minchinton and Tannock, 2006). In future studies, it would be interesting to determine the actual concentration of drugs like Dox at poorly perfused tumor areas to determine whether different p53 target genes show an inverse expression pattern dependent on Dox concentration. The naturally fluorescent nature of Dox offers a convenient method to detect the spatial distribution of Dox perfusion in tumor tissue (Coley et al., 1993).

Our results also show the importance of the effective dose of a given drug in a tumor because as little as a 2-fold dose change can have a dramatic effect on protein expression and cell outcome (Figure 4D). Moreover, because these differences may not be manifested at the transcriptome level, the use of transcriptomic analysis to determine the effects of drugs on cells should ideally be coupled with proteomic analysis to offer a clearer, more comprehensive picture of gene expression. Future experiments analyzing the effects of different doses of chemotherapeutic agents such as Dox could yield valuable insight into the heterogeneous effects that likely characterize the treatment of solid tumors. Moreover, our findings reinforce the importance of identifying methods that increase the local concentration of chemotherapeutic agents throughout the tumor without requiring systemic dose increases, especially because drugs such as Dox can cause secondary cancers or cardiotoxicity when administered in high doses.

In conclusion, in addition to identification of the endocytic receptor LRP1 as a p53 target, we show evidence of a dose-dependent regulatory mechanism of LRP1 expression that occurs at the post-transcriptional level. Our results show that, although lethal doses of commonly used chemotherapeutic agents can induce transcript expression of LRP1, a p53-driven miRNA feedback loop prevents the translation of LRP1 transcripts, which promotes cell death. We anticipate that future studies of p53-regulated genes could yield several more p53 targets that are regulated in a similar manner.

EXPERIMENTAL PROCEDURES

Cell Lines and Reagents

HCT116 WT and $p53^{-/-}$ cells, all HCT116 derivatives, and H1299, MCF-7, and U2OS cells were cultured in DMEM supplemented with 10% fetal bovine serum (FBS) at 37°C in the presence of 5% CO_2. MG132 was purchased from Calbiochem (catalog no. 474790). Cycloheximide (catalog no. C7698), Dox (D1515), CQ (C6628), Etop (E1383), ActD (A9415), and nutlin-3a (SML0580) were purchased from Sigma. MiR-103–3p (470828–001) and miR-107 (470827–001) mimics were purchased from Exiqon. MiR-103–3p (IH-300522–05-0002) and miR-107 (IH-300527–05-0002) antagomirs were purchased from Dharmacon. 5FU and cisplatin were obtained from the University of North Carolina (UNC) pharmacy. QVD was purchased from Thermo Fisher Scientific. Phusion polymerase (catalog no. M0530S) and all restriction enzymes were purchased from New England Biolabs. Effectene transfection reagent was purchased from QIAGEN. Anti-LRP1 antibody recognizing the β-subunit of LRP1 was purchased from Abcam (ab92544, Cambridge, UK). Polyclonal anti-LRP1 antibody was generously provided by the Herz laboratory at University of Texas-Southwestern. Mouse anti-actin (MAB1501, Chemicon), mouse anti-p53 (DO-1, Labvision AB-6, catalog no. MS-187P), goat anti-p21 (C19, SC-397G, Santa Cruz Biotechnology), mouse anti-PARP (clone C2–10, 556362, BD Biosciences), rabbit anti-cleaved caspase-3 (D175, 9661S, Cell Signaling Technology), and rat anti-APAF1 (ALX-804–348-C100; Enzo Life Sciences) antibodies were purchased. miRNA assays, the miRNA reverse transcription kit, and TaqMan miRNA Universal PCR Master Mix were ordered from Thermo Fisher Scientific. Oligonucleotides for cloning, PCR, or reverse transcription were ordered through the UNC Nucleic Acid Core Facility. For Dox treatments, pulsed Dox (a sub-lethal dose of Dox) refers to the treatment of cells for 1 hr with 1 μM Dox followed by a PBS wash and fresh DMEM. High Dox refers to treating cells with a constant 1-μM dose of Dox for 24 hr unless specified otherwise.

Mimic and Antagomir Transfection

Cells were plated at 50% confluency, after which cells were transfected with 40 μM mimic or antagomir as indicated using the recommended RNAiMAX transfection protocol. Cells were then treated for an additional 24 h or harvested and analyzed.

qRT-PCR

After treatment, RNA was purified from cells using the Zymo Quick RNA mini-prep kit according to the protocol recommended by the manufacturer (Zymo Research, catalog no. R1057). Then cDNA was synthesized using a Bio-Rad iScript cDNA synthesis kit (catalog no. 1708891) for total RNA or a TaqMan miRNA reverse transcription kit for miRNA (Thermo Fisher Scientific, catalog no. 4366596). cDNA was analyzed using SYBR Green reagent (Bio-Rad, catalog no. 1525271) or TaqMan assays (Thermo Fisher Scientific, catalog no. 4427975 [all human]: miR-205–5p, assay ID000509; miR-200b-3p, 002251; miR-200c-3p, 002300; miR-103–3p, 000439; miR-107, 000443; U6, 001973) according to the protocol recommended by the manufacturer. Data were analyzed using the $\Delta\Delta C_t$ method, and experiments were normalized to actin, glyceraldehyde 3-phosphate dehydrogenase (GAPDH), or U6 miRNA. Primer sequences included the following: LRP1: forward (Fwd)

5′-CAACAGATCAAC GACGATGG-3′, reverse (Rev) 5′-GGGTGGCGTCAGAGAAGTAG-3′; PUMA: Fwd 5′-ACGACCTCAACGCACAGTACG-3′, Rev 5′-GTAAGGGCAGGAGT CCCATGATG-3′; Apaf1: Fwd 5′-GGAGGACCCTCAAGAGGATATG-3′, Rev 5′-GGATTTCTCCCAATAGGCCACT-3′; Noxa: Fwd 5′-AGAAGGCGCGCAAGAAC-3′, Rev 5′-GCACCTTCACATTCCTCTCAG-3′; CDKN1A: Fwd 5′-GTCAGAACCCATGCGGCAGCAAG-3′, Rev 5′-CAGGTCCACATGGTCTTCCTC TG-3′; Actin Fwd 5′-AGAAAATCTGGCACCACACC-3′, Rev 5′-CTCCTTAA TGTCACGCACGA-3′; GAPDH Fwd 5′-CCTGACCTGCCGTCTAGAAAAA CCT-3′, Rev 5′-CCATGAGGTCCACCACCCTGTT-3′.

Luciferase Assay

The WT or a mutant version of the p53 RE for LRP1 was cloned into the pGL3 basic vector. The resultant construct was co-transfected into p53-null H1299 cells in 6-well plates along with a constitutive *Renilla* luciferase expression construct and either empty vector or a p53-expressing construct. A positive Ctrl construct harboring the native p21 p53 RE was included. Transfection was conducted for 24 hr, after which the cells were analyzed for luciferase signal using a Promega DualGlo Luciferase kit (Promega, Madison, WI) according to the protocol recommended by the manufacturer. Briefly, after transfection, cells were trypsinized and transferred to 96-well plates. Cells were lysed with equal volumes of DualGlo reagent, and then the firefly luciferase signal was determined using a SpectraMax plate reader. Next, one volume of Stop & Glo reagent was added to each well, and the wells were read for the *Renilla* luciferase signal. For analysis, the firefly luciferase signal was normalized to the corresponding *Renilla* luciferase signal. After normalization, the luciferase signal in the presence of WT p53 was normalized to the luciferase signal in the presence of the empty vector. Data represent the averages and SD of two independent experiments performed in triplicate. The following oligonucleotides were annealed to construct the luciferase vectors: LRP1 Fwd 5′-TCGAGGAGCCCCACGCGGGC GGACAAGCTCCGGCGTGTCCCCTCGG GTGTCCCTGA-3′, Rev 5′-AGCTTCAGGGACACCCGAGG GGACACGCCGGAGCTTGTCCGCCCGCGTGGGGCTCC-3′; LRP1 mutant Fwd 5′-TCGAGGAGCCCCACGCGGGCGGATAATCTCCGGAGTATCCCCTCGGGTGTCCCTG A-3′, Rev 5′-AGCTTCAGGGACACCCGAGGGGATACTCCGGAGATTATCC GCCCGCGTGGGGCTCC-3′; p21 Fwd 5′-CAGGGTACCGCTTTCTGGCCGT CAGGAACATGTCCCAACATGTTGAGCTCTGGCAAGCTTGAC-3′, Rev 5′-GT CAAGCTTGCCAGAGCTCAACATGTTGGGACATGTTCCTGACGGCCAGAAA GCGGTACCCTG-3′. The p53 R273H mutant construct was made using site-directed mutagenesis (SDM) based on a pcDNA3-WT p53 vector using the following primers: Fwd 5′-GGAACAGCTTTGAGGTGCATGTTTGTGCCTGT CCTGG-3′, Rev 5′-CCAGGACAGGCACAAACATGCACCTCAAAGCTGTT CC-3′. The miR-103/107 seed region mutants were generated based on a WT luciferase construct containing the WT LRP1 3′ UTR ordered from Genecopoeia (catalog no. HmiT010870-MT06). The SDM primers used were as follows: Fwd 5′-TCCTTGGCACCCCCATAATACCTTCAGGGAGA CAGGCAG-3′, Rev 5′-CTGCCTGTCTCCCTGAAGGTATTATGGGGGTGCCAA GGA-3′.

CRISPR/Cas9 Deletion

CRISPR/Cas9 constructs were designed and assembled based on previous reports (Cong et al., 2013). Briefly, high-scoring guide RNAs (gRNAs) were identified using the CRISPR design tool developed by the Feng Zhang lab. LRP1 exons 1, 2, and 3 and p53 exons 3 and 5 were used as input to identify gRNAs, and the gRNAs were synthesized, annealed, and cloned into the PX260 plasmid. gRNA-annealed oligonucleotides included the following: LRP1 exon1: Fwd 5′-CACCGGCTCTCAGCTCTGGTCGCGG-3′, Rev 5′-AAA CCCGCGACCAGAGCTGAGAGCC-3′; LRP1 exon2: Fwd 5′-CACCGTCAAAG GGCTGGCGGTGCGA-3′, Rev 5′-AAACTCGCACCGCCAGCCCTTTGAC-3′; LRP1 exon3: Fwd 5′-CACCGGCTCGTTTGGCTGGCATCGC-3′, Rev 5′-AAA CGCGATGCCAGCCAAACGAGCC-3′; p53 exon3 Fwd 5′-CACCGTCCTCAG CATCTTATCCGAG-3′, Rev 5′-AAACCTCGGATAAGATGCTGAGGAC-3′; p53 exon5 Fwd 5′-CACCGCCATTGTTCAATATCGTCCG-3′, Rev 5′-AAACCGGA CGATATTGAACAATGGC-3′. The CRISPR constructs were transfected into cells for 24 hr and selected with puromycin for 72 hr. After selection, individual clones were isolated using limiting dilution. After 2 weeks, colonies were screened for the absence of LRP1 or p53, and KO clones were used for subsequent analyses.

SiRNA Treatment

HCT116 cells were plated at 40% confluency in 6-well plates, after which the cells were transfected with siLRP1 or siCtrl duplexes (40 μM; Sigma, St.Louis, MO) using RNAiMAX according to the protocol recommended by the manufacturer. The transfection was conducted for either 72 hr or for the indicated amount of time before the cells were collected and analyzed. The following small interfering RNA (siRNA) constructs were used (sense strand displayed): siCtrl, 5′-CAG UCGCGUUUGCGACUGG[dT][dT]-3′; siLRP1–1, 5′-GACUUGCAGCCCCAAG CAGUU[dT][dT]-3′; siLRP1–2, 5′-GCAGUUUGCCUGCAGAGAUUU[dT][dT]-3′.

ChIP

ChIP assays were conducted using the QuickChIP kit (Novus Biologicals, Littleton, CO) according to the protocol recommended by the manufacturer with a few adaptations for p53 immunoprecipitation. HCT116 cells were grown and treated in 10-cm dishes, after which cells were incubated with 1% formalin at 37°C for 10 min. Formalin was neutralized with glycine, and then the cells were washed twice with cold PBS. Cells were scraped in cold PBS, pelleted, and resuspended in 1 mL of SDS lysis buffer. DNA was sonicated and then precleared with protein-A/G agarose beads. Precleared DNA was subjected to immunoprecipitation (IP) with 0.6 μg of p53 antibody by rotating at 4°C overnight. Antibody-p53/DNA complexes were pulled down by incubation with protein A/G beads at 4°C for 1 hr. Beads were washed, and then p53-DNA complexes were eluted from the beads. Cross-links were reversed with 200 mM NaCl incubated at 65°C overnight. Samples were RNase-treated and then incubated with 10 mM EDTA, 25 mM Tris-HCl (pH 6.5), and 20 μg/μL proteinase K for 1hr at 45°C. DNA was purified using a QIAGEN PCR purification kit, and then DNA was quantified using qPCR. Primers for ChIP qPCR included the following: LRP1 p53RE: Fwd 5′-AATGAGCCCCGACTTCTTG-3′, Rev 5′-TCGGAGTAAA

CAGGGACACC-3′; p21 p53RE: Fwd 5′-CTGGACTGGGCACTCTTGTC-3′, Rev 5′-CTCCTACCATCCCCTTCCTC-3′.

^{35}Cys/^{35}Met Labeling Assay

Cells were treated in 6-cm dishes for 24 hr. Then cells were starved with Cys/ Met-free DMEM for 30 min, after which 170 μCi of ^{35}Cys/^{35}Met was added to each dish. Cycloheximide was included in one sample to Ctrl for *de novo* translation-mediated incorporation of the ^{35}S label. The label was applied for 30 min, followed by a 30-min chase period with complete DMEM. Then cells were lysed in 0.1% NP-40 lysis buffer containing inhibitors. Lysates were subjected to IP using an anti-LRP1 antibody (ab92544, Abcam, Cambridge, UK). After separation on 10% SDS-PAGE gels, the gels were dried for 4 hr on a vacuum gel drying apparatus, and then the gel was exposed to autoradiography film. Immunoprecipitated protein was normalized to the respective input lanes using ImageJ densitometry analysis.

Comet Assay

The protocol used for the comet assay has been reported previously (Speit and Hartmann, 2006). Briefly, HCT116 cells were treated with Dox. Then the cells were collected, embedded in low-melting point agarose, and mounted onto slides (1×10^4 cells/slide). Cells were lysed, subjected to electrophoretic migration, neutralized, and then stained with ethidium bromide. Cells were imaged using an Olympus IX81 fluorescence microscope fitted with a SPOT camera.

Statistical Analysis

All statistical analyses were conducted using GraphPad Prism software version 5.0 (GraphPad, La Jolla, CA). Comparisons between two groups were conducted using Student's unpaired t tests. Data are presented as the means ± SD. $p < 0.05$ was considered statistically significant. *, **, and *** correspond to $p < 0.05$, 0.01, and 0.001, respectively.

Supplementary Material

Refer to Web version on PubMed Central for supplementary material.

ACKNOWLEDGMENTS

The authors thank Dr. Nicole Tackmann for technical assistance with flow cytometry cell cycle analysis, Dr. Joachim Herz for generously providing the polyclonal anti-LRP1 antibody, and Dr. Praveen Sethupathy and Lisa Kurtz for assistance with the miRNA analysis. This study was funded, in part or in whole, by the following sources: National Cancer Institute grants (CA127770, CA100302, CA167637, and CA155235, all to Y.Z.), a fellowship from the University of North Carolina Genetics and Molecular Biology Training (grant 5T32 GM007092 to P.L.L.), and grants from the NSFC (81672618) and Jiangsu Center for the Collaboration and Innovation of Cancer Biotherapy (to Y.L.).

REFERENCES

Bertheau P, Lehmann-Che J, Varna M, Dumay A, Poirot B, Porcher R, Turpin E, Plassa LF, de Roquancourt A, Bourstyn E, et al. (2013). p53 in breast cancer subtypes and new insights into response to chemotherapy. Breast 22 (Suppl 2), S27–S29. [PubMed: 24074787]

Campana WM, Li X, Dragojlovic N, Janes J, Gaultier A, and Gonias SL (2006). The low-density lipoprotein receptor-related protein is a pro-survival receptor in Schwann cells: possible implications in peripheral nerve injury. J. Neurosci 26, 11197–11207. [PubMed: 17065459]

Ceschin DG, Sánchez MC, and Chiabrando GA (2009). Insulin induces the low density lipoprotein receptor-related protein 1 (LRP1) degradation by the proteasomal system in J774 macrophage-derived cells. J. Cell. Biochem 106, 372–380. [PubMed: 19115269]

Chang BD, Broude EV, Dokmanovic M, Zhu H, Ruth A, Xuan Y, Kandel ES, Lausch E, Christov K, and Roninson IB (1999). A senescence-like phenotype distinguishes tumor cells that undergo terminal proliferation arrest after exposure to anticancer agents. Cancer Res. 59, 3761–3767. [PubMed: 10446993]

Chang TC, Wentzel EA, Kent OA, Ramachandran K, Mullendore M, Lee KH, Feldmann G, Yamakuchi M, Ferlito M, Lowenstein CJ, et al. (2007). Transactivation of miR-34a by p53 broadly influences gene expression and promotes apoptosis. Mol. Cell 26, 745–752. [PubMed: 17540599]

Chen Q, Xu J, Li L, Li H, Mao S, Zhang F, Zen K, Zhang CY, and Zhang Q (2014). MicroRNA-23a/b and microRNA-27a/b suppress Apaf-1 protein and alleviate hypoxia-induced neuronal apoptosis. Cell Death Dis. 5, e1132. [PubMed: 24651435]

Coley HM, Amos WB, Twentyman PR, and Workman P (1993). Examination by laser scanning confocal fluorescence imaging microscopy of the subcellular localisation of anthracyclines in parent and multidrug resistant cell lines. Br. J. Cancer 67, 1316–1323. [PubMed: 8099807]

Cong L, Ran FA, Cox D, Lin S, Barretto R, Habib N, Hsu PD, Wu X, Jiang W, Marraffini LA, and Zhang F (2013). Multiplex genome engineering using CRISPR/Cas systems. Science 339, 819–823. [PubMed: 23287718]

Deisenroth C, Itahana Y, Tollini L, Jin A, and Zhang Y (2011). p53-Inducible DHRS3 is an endoplasmic reticulum protein associated with lipid droplet accumulation. J. Biol. Chem 286, 28343–28356. [PubMed: 21659514]

Franklin DA, He Y, Leslie PL, Tikunov AP, Fenger N, Macdonald JM, and Zhang Y (2016). p53 coordinates DNA repair with nucleotide synthesis by suppressing PFKFB3 expression and promoting the pentose phosphate pathway. Sci. Rep 6, 38067. [PubMed: 27901115]

Fuentealba RA, Liu Q, Kanekiyo T, Zhang J, and Bu G (2009). Low density lipoprotein receptor-related protein 1 promotes anti-apoptotic signaling in neurons by activating Akt survival pathway. J. Biol. Chem 284, 34045–34053. [PubMed: 19815552]

Gonias SL, and Campana WM (2014). LDL receptor-related protein-1: a regulator of inflammation in atherosclerosis, cancer, and injury to the nervous system. Am. J. Pathol 184, 18–27. [PubMed: 24128688]

Hamlin AN, Basford JE, Jaeschke A, and Hui DY (2016). LRP1 Protein Deficiency Exacerbates Palmitate-induced Steatosis and Toxicity in Hepatocytes. J. Biol. Chem 291, 16610–16619. [PubMed: 27317662]

Hermeking H (2012). MicroRNAs in the p53 network: micromanagement of tumour suppression. Nat. Rev. Cancer 12, 613–626. [PubMed: 22898542]

Hollstein M, Sidransky D, Vogelstein B, and Harris CC (1991). p53 mutations in human cancers. Science 253, 49–53. [PubMed: 1905840]

Huang S, Shu L, Dilling MB, Easton J, Harwood FC, Ichijo H, and Houghton PJ (2003). Sustained activation of the JNK cascade and rapamycin-induced apoptosis are suppressed by p53/p21(Cip1). Mol. Cell 11, 1491–1501. [PubMed: 12820963]

Jackson JG, Pant V, Li Q, Chang LL, Quintás-Cardama A, Garza D, Tavana O, Yang P, Manshouri T, Li Y, et al. (2012). p53-mediated senescence impairs the apoptotic response to chemotherapy and clinical outcome in breast cancer. Cancer Cell 21, 793–806. [PubMed: 22698404]

Koutsodontis G, Vasilaki E, Chou WC, Papakosta P, and Kardassis D (2005). Physical and functional interactions between members of the tumour suppressor p53 and the Sp families of transcription factors: importance for the regulation of genes involved in cell-cycle arrest and apoptosis. Biochem. J 389, 443–455. [PubMed: 15790310]

Kracikova M, Akiri G, George A, Sachidanandam R, and Aaronson SA (2013). A threshold mechanism mediates p53 cell fate decision between growth arrest and apoptosis. Cell Death Differ. 20, 576–588. [PubMed: 23306555]

Kruiswijk F, Labuschagne CF, and Vousden KH (2015). p53 in survival, death and metabolic health: a lifeguard with a licence to kill. Nat. Rev. Mol. Cell Biol 16, 393–405. [PubMed: 26122615]

Leslie PL, and Zhang Y (2016). MDM2 oligomers: antagonizers of the guardian of the genome. Oncogene 35, 6157–6165. [PubMed: 27041565]

Lleó A, Waldron E, von Arnim CA, Herl L, Tangredi MM, Peltan ID, Strickland DK, Koo EH, Hyman BT, Pietrzik CU, and Berezovska O (2005). Low density lipoprotein receptor-related protein (LRP) interacts with presenilin 1 and is a competitive substrate of the amyloid precursor protein (APP) for gamma-secretase. J. Biol. Chem 280, 27303–27309. [PubMed: 15917251]

Mahyar-Roemer M, and Roemer K (2001). p21 Waf1/Cip1 can protect human colon carcinoma cells against p53-dependent and p53-independent apoptosis induced by natural chemopreventive and therapeutic agents. Oncogene 20, 3387–3398. [PubMed: 11423989]

Martins CP, Brown-Swigart L, and Evan GI (2006). Modeling the therapeutic efficacy of p53 restoration in tumors. Cell 127, 1323–1334. [PubMed: 17182091]

May P, Reddy YK, and Herz J (2002). Proteolytic processing of low density lipoprotein receptor-related protein mediates regulated release of its intracellular domain. J. Biol. Chem 277, 18736–18743. [PubMed: 11907044]

Minchinton AI, and Tannock IF (2006). Drug penetration in solid tumours. Nat. Rev. Cancer 6, 583–592. [PubMed: 16862189]

Paek AL, Liu JC, Loewer A, Forrester WC, and Lahav G (2016). Cell-to-Cell Variation in p53 Dynamics Leads to Fractional Killing. Cell 165, 631–642. [PubMed: 27062928]

Piovan C, Palmieri D, Di Leva G, Braccioli L, Casalini P, Nuovo G, Tortoreto M, Sasso M, Plantamura I, Triulzi T, et al. (2012). Oncosuppressive role of p53-induced miR-205 in triple negative breast cancer. Mol. Oncol 6, 458–472. [PubMed: 22578566]

Purvis JE, Karhohs KW, Mock C, Batchelor E, Loewer A, and Lahav G (2012). p53 dynamics control cell fate. Science 336, 1440–1444. [PubMed: 22700930]

Rinaldo C, Prodosmo A, Mancini F, Iacovelli S, Sacchi A, Moretti F, and Soddu S (2007). MDM2-regulated degradation of HIPK2 prevents p53Ser46 phosphorylation and DNA damage-induced apoptosis. Mol. Cell 25, 739–750. [PubMed: 17349959]

Sohn D, Essmann F, Schulze-Osthoff K, and Jänicke RU (2006). p21 blocks irradiation-induced apoptosis downstream of mitochondria by inhibition of cyclin-dependent kinase-mediated caspase-9 activation. Cancer Res. 66, 11254–11262. [PubMed: 17145870]

Speit G, and Hartmann A (2006). The comet assay: a sensitive genotoxicity test for the detection of DNA damage and repair. Methods Mol. Biol 314, 275–286. [PubMed: 16673888]

Suzuki A, Tsutomi Y, Akahane K, Araki T, and Miura M (1998). Resistance to Fas-mediated apoptosis: activation of caspase 3 is regulated by cell cycle regulator p21WAF1 and IAP gene family ILP. Oncogene 17, 931–939. [PubMed: 9747872]

Szak ST, Mays D, and Pietenpol JA (2001). Kinetics of p53 binding to promoter sites in vivo. Mol. Cell. Biol 21, 3375–3386. [PubMed: 11313463]

Ventura A, Kirsch DG, McLaughlin ME, Tuveson DA, Grimm J, Lintault L, Newman J, Reczek EE, Weissleder R, and Jacks T (2007). Restoration of p53 function leads to tumour regression in vivo. Nature 445, 661–665. [PubMed: 17251932]

von Arnim CA, Kinoshita A, Peltan ID, Tangredi MM, Herl L, Lee BM, Spoelgen R, Hshieh TT, Ranganathan S, Battey FD, et al. (2005). The low density lipoprotein receptor-related protein (LRP) is a novel beta-secretase (BACE1) substrate. J. Biol. Chem 280, 17777–17785. [PubMed: 15749709]

Waldman T, Lengauer C, Kinzler KW, and Vogelstein B (1996). Uncoupling of S phase and mitosis induced by anticancer agents in cells lacking p21. Nature 381, 713–716. [PubMed: 8649519]

Wang B, Xiao Z, and Ren EC (2009). Redefining the p53 response element. Proc. Natl. Acad. Sci. USA 106, 14373–14378. [PubMed: 19597154]

Weinberg RL, Veprintsev DB, Bycroft M, and Fersht AR (2005). Comparative binding of p53 to its promoter and DNA recognition elements. J. Mol. Biol 348, 589–596. [PubMed: 15826656]

Xue W, Zender L, Miething C, Dickins RA, Hernando E, Krizhanovsky V, Cordon-Cardo C, and Lowe SW (2007). Senescence and tumour clearance is triggered by p53 restoration in murine liver carcinomas. Nature 445, 656–660. [PubMed: 17251933]

Yamakuchi M, Lotterman CD, Bao C, Hruban RH, Karim B, Mendell JT, Huso D, and Lowenstein CJ (2010). P53-induced microRNA-107 inhibits HIF-1 and tumor angiogenesis. Proc. Natl. Acad. Sci. USA 107, 6334–6339. [PubMed: 20308559]

Highlights

- LRP1 is a p53 target whose transcription is upregulated in response to stresses
- Lethal doses of stress induce p53-regulated miRNAs miR-103 and miR-107
- miR-103 and miR-107 inhibit LRP1 translation through a feedback loop
- LRP1 suppression by miR-103 and miR-107 promotes cancer cell death

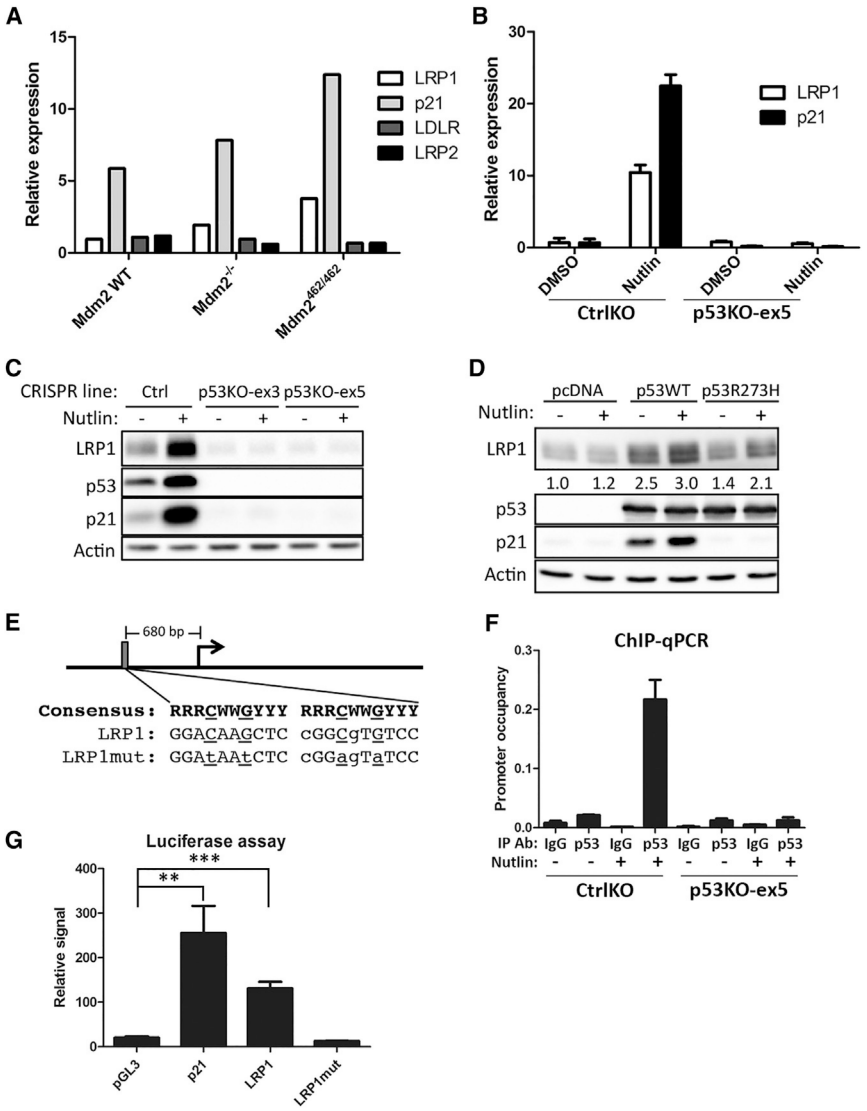

Figure 1. LRP1 Is a Direct p53 Target Gene

(A) Microarray screen of Mdm2$^{WT/WT}$, Mdm2$^{-/-}$, and Mdm2$^{462/462}$ MEF cells reveals a similar expression pattern between LRP1 and p21. The Ctrl genes LDLR and LRP2 do not show increasing expression patterns.

(B) The LRP1 transcript shows a p53-dependent increase in expression. CRISPR Ctrl or p53 knockout cells (p53KO) were treated with vehicle or 10 μM nutlin-3a. Data represent samples run in triplicate in at least two biological replicates.

(C) LRP1 protein shows a p53-dependent increase in expression. CRISPR Ctrl or p53 KO cells (single guide RNAs [sgRNAs] targeting exon 3 or 5) were treated as in (B). Data represent at least two biological replicates. </p/>(D) WT p53 rescues LRP1 expression. H1299 cells were transfected with WT or mutant (R273H) p53 for 24 hr, after which the cells were treated with vehicle or 10 μM nutlin-3a for 24 hr. Data represent at least two biological replicates.

(E) A putative p53 RE was identified in close proximity to the LRP1 transcription start site.

(F) p53 binds directly to the putative p53 RE in the LRP1 promoter. p53 isogenic HCT116 cells were treated with vehicle or 10 μM nutlin-3a for 24 hr, after which the cells were subjected to ChIP with p53 antibody or non-specific immunoglobulin G (IgG). Data represent samples run in triplicate in at least two biological replicates.
(G) The LRP1 p53 RE is sufficient to drive reporter gene expression. H1299 cells were transiently transfected with luciferase plasmids containing the endogenous WT LRP1 p53 RE or a mutated derivative of the LRP1 p53 RE. The p21 WT p53 RE was included as a positive Ctrl. Data were normalized to the *Renilla* luciferase signal, and the data are presented as the luciferase signal in the presence of WT p53 relative to the signal in the absence of p53. Data are compiled results from samples run in triplicate in at least two biological replicates. **$p < 0.01$.

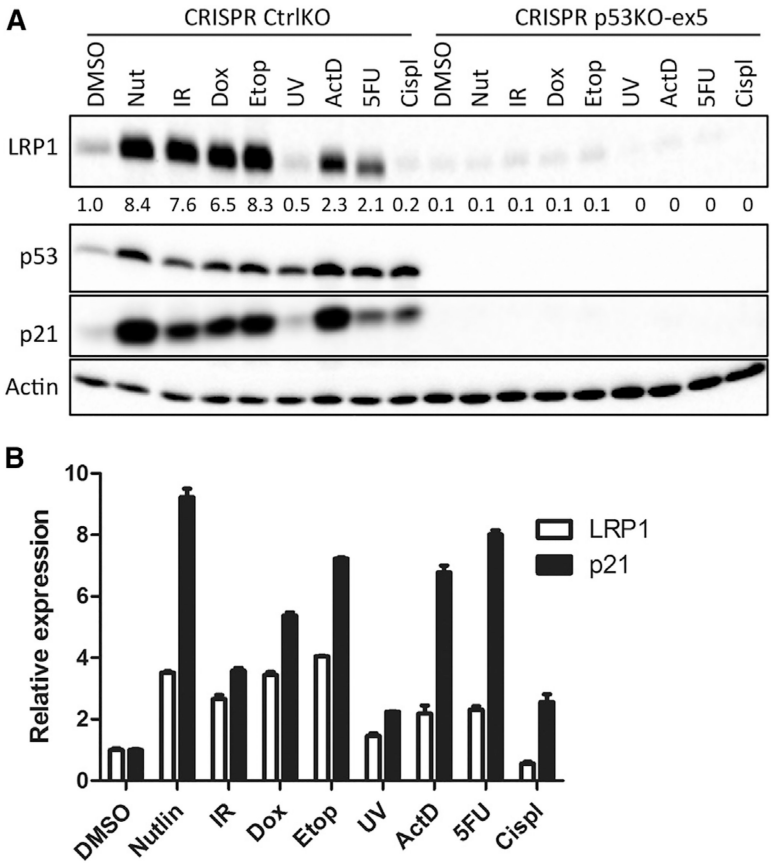

Figure 2. LRP1 Is Induced in Response to Canonical p53-Activating Stresses

(A) LRP1 protein is expressed in response to several types of stress. HCT116 CRISPR Ctrl or p53 KO cells were treated with the indicated stresses for 24 hr and then probed for the indicated proteins. Data represent at least two biological replicates.

(B) HCT116 cells were treated with the indicated stresses for 24 hr, after which transcript levels were evaluated. Treatment abbreviations: Nut, 10 μM nutlin-3a; IR, 10 Gy ionizing radiation; Dox, 200 nM doxorubicin; Etop, 10 μM etoposide; UV, 25 J/m^2 UV-C; ActD, 5 nM actinomycin D; 5FU, 100 μM 5-fluorouracil; Cispl, 10 μM cisplatin. Data represent at least two biological replicates, each of which was run in triplicate.

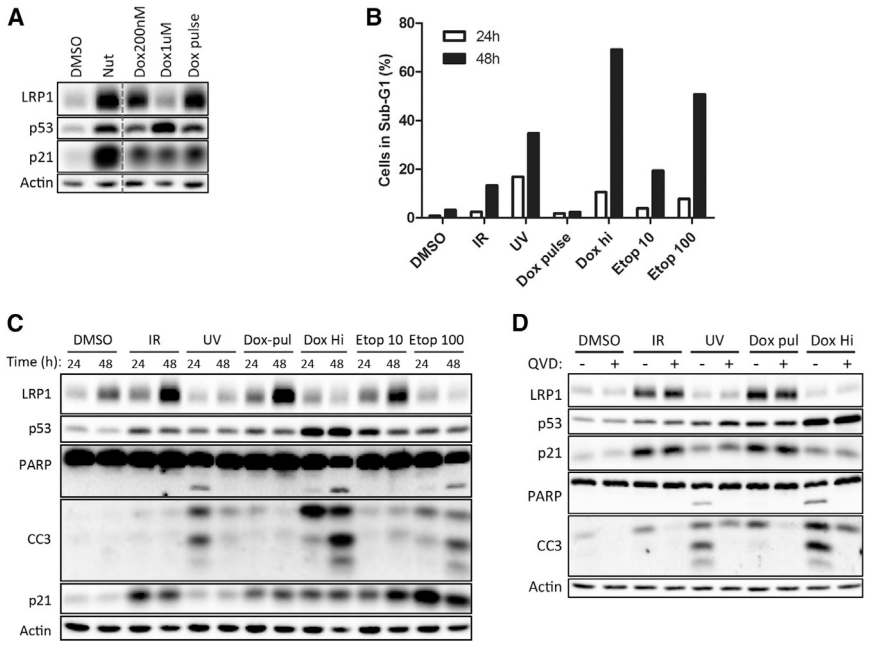

Figure 3. LRP1 Protein Is Expressed in Response to Sub-lethal Stresses

(A) HCT116 cells were treated with sub-lethal (200 nM or 1 hr of 1 μM) or lethal (1 μM constant) Dox for 24 hr, after which the samples were analyzed by western blotting. Data represent at least two biological replicates.

(B) HCT116 cells were treated with the indicated stress for 24 or 48 hr, after which the cells were subjected to propidium iodide (PI) staining and flow cytometry analysis. The percentages of sub-G1 cells are quantified in the graph. Data represent at least two biological replicates.

(C) The HCT116 protein lysates from (B) were subjected to western blot analysis. Data represent at least two biological replicates.

(D) HCT116 cells were treated with the indicated stresses in the presence or absence of the caspase inhibitor QVD, 24 hr after which lysates were subjected to western blot analysis. Treatment abbreviations: Dox pulse and Dox hi, see Experimental Procedures. Data represent at least two biological replicates.

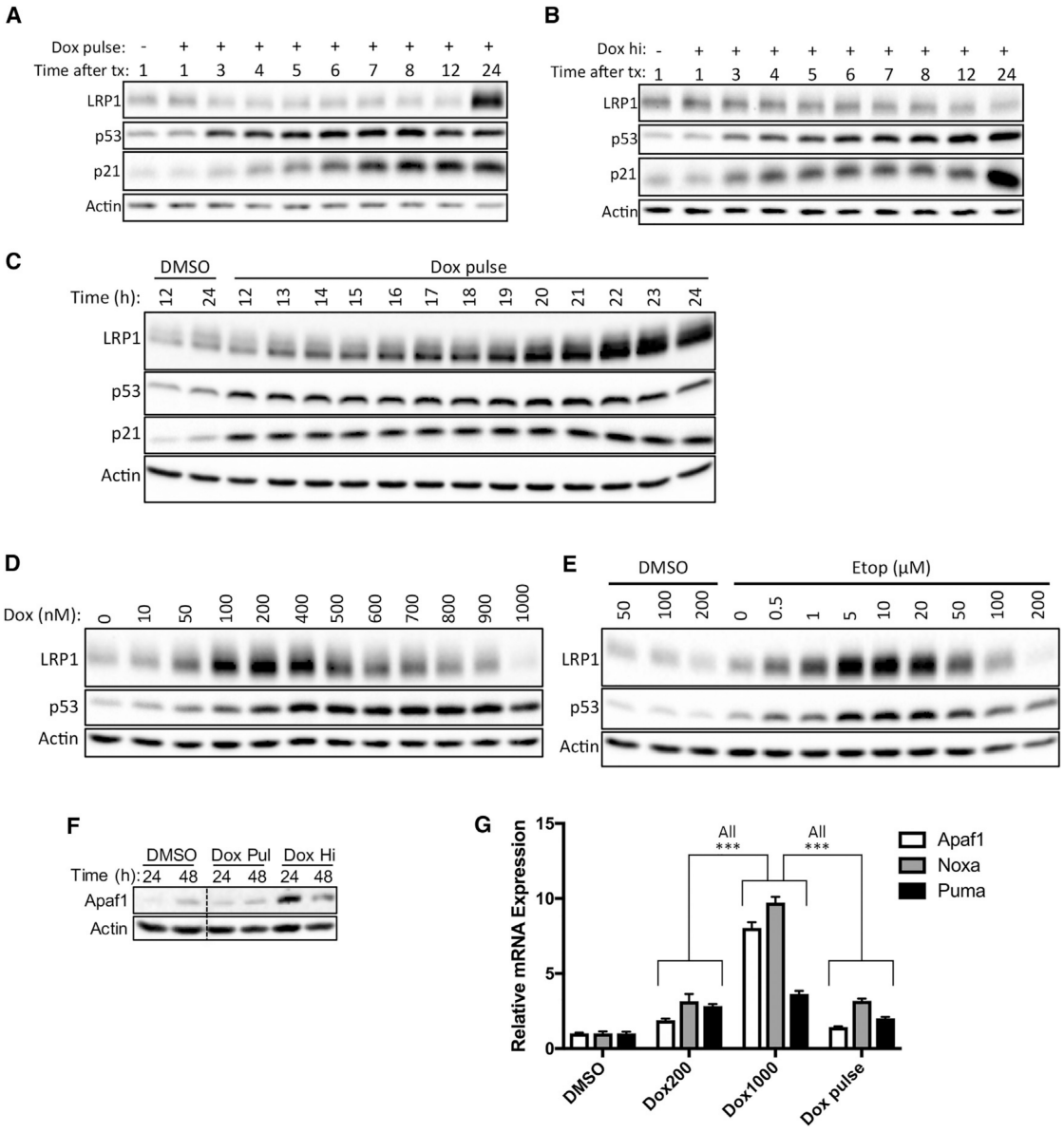

Figure 4. Sub-lethal but Not Lethal Dox Induces LRP1 Protein Expression

(A) HCT116 cells were treated with 1 μM Dox for 1 hr, after which the drug was withdrawn, and the cells were cultured for an additional amount of time as indicated. Data represent at least two biological replicates.

(B) HCT116 cells were treated with 1 μM Dox for the indicated amount of time, at which point lysates were collected and analyzed by western blotting. Data represent at least two biological replicates.

(C) HCT116 cells were subjected to a more detailed time course experiment between 12 and 24 hr after Dox pulse treatment. Data represent at least two biological replicates.

(D) HCT116 cells were treated with the indicated dose of Dox for 24 hr, after which lysates were collected and analyzed by western blot. Data represent at least two biological replicates.

(E) HCT116 cells were treated with the indicated dose of Etop for 24 hr, after which lysates were collected and analyzed by western blot. Data represent at least two biological replicates.

(F) HCT116 cells were treated for 24 or 48 hr with vehicle or the indicated dose of Dox, after which protein lysates were generated and subjected to western blotting. Data represent at least two biological replicates.

(G) HCT116 cells were treated with the indicated dose of Dox for 24 hr, after which RNA was purified and subjected to analysis for the indicated pro-apoptotic p53 target genes. Data represent at least two biological replicates, each performed in triplicate. ***$p < 0.001$.

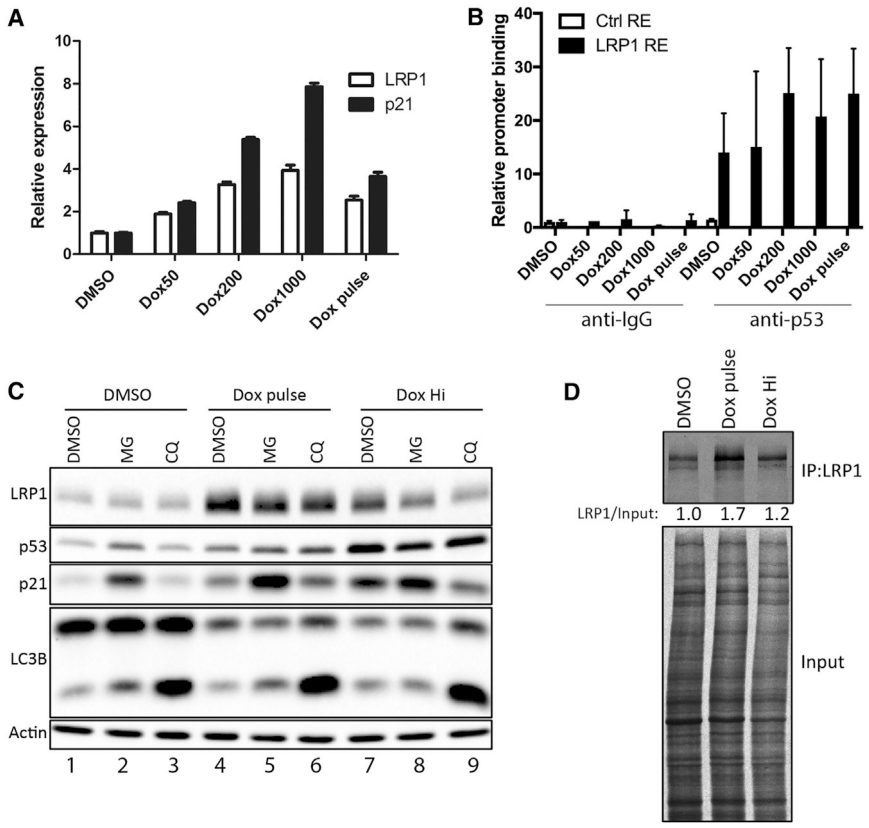

Figure 5. Lethal Dox Suppresses LRP1 Protein Translation through the p53-Regulated miRNAs MiR-103 and MiR-107

(A) HCT116 cells were treated with the indicated dose of Dox (nanomolar) for 24 hr, after which RNA was collected and subjected to qRT-PCR analysis. Data represent at least two biological replicates, each performed in triplicate.

(B) HCT116 cells were treated with the indicated dose of Dox for 24 hr, after which cells were subjected to ChIP analysis using anti-p53 antibody and non-specific IgG. Data represent at least two biological replicates, each performed in triplicate.

(C) HCT116 cells were treated with the indicated stress for 24 hr, after which vehicle, MG132 (MG), or CQ was added to the cells for an additional 8 hr. After MG or CQ treatment, lysates were collected and subjected to western blot analysis. Data represent at least two biological replicates.

(D) HCT116 cells were treated with the indicated course of Dox for 24 hr, after which cells were labeled with ^{35}S-Met/Cys for 30 min, chased with complete DMEM for another 30 min, and then subjected to LRP1 immunoprecipitation. Data represent at least two biological replicates.

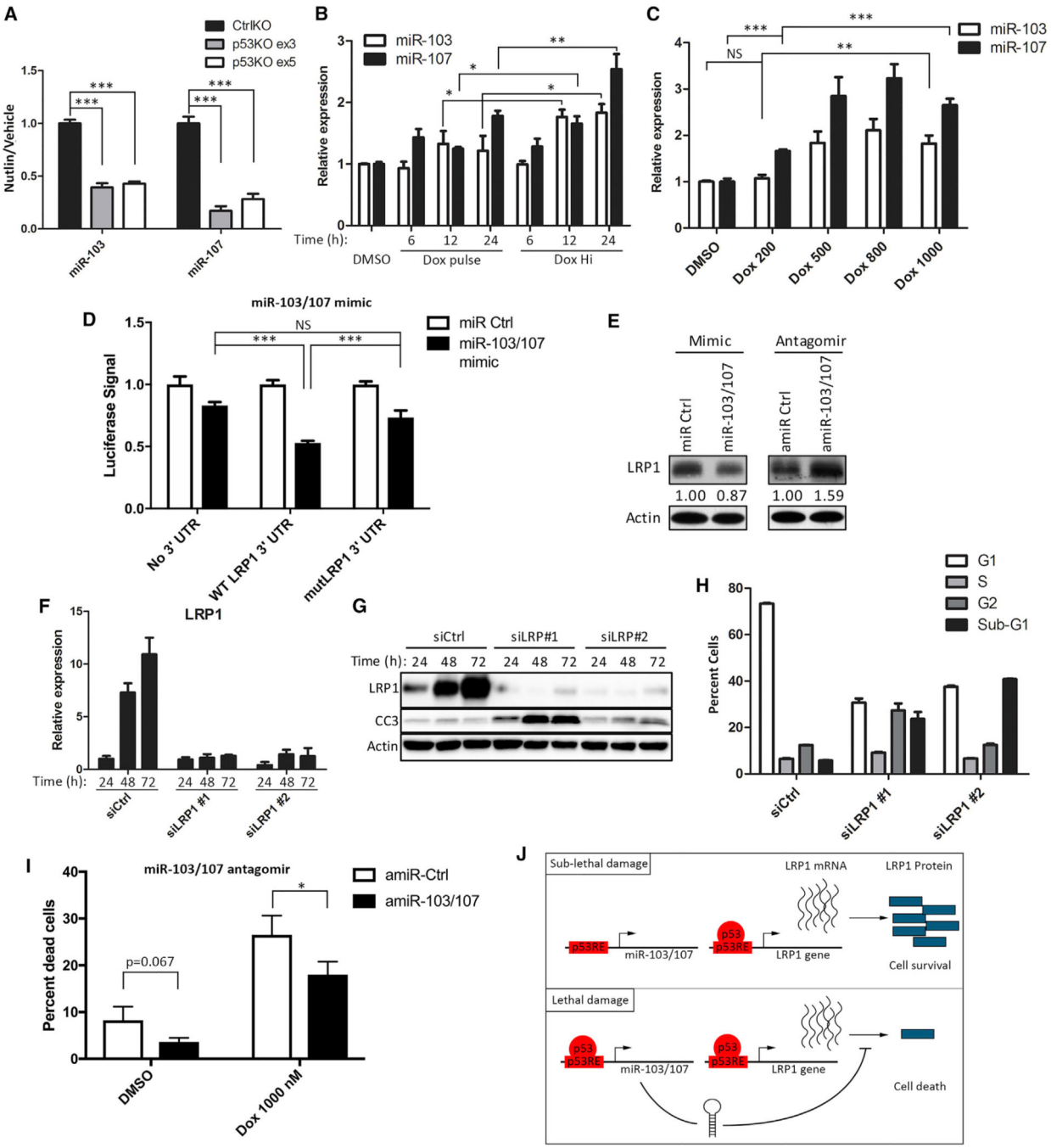

Figure 6. Lethal Stress but Not Sub-lethal Stress Induces the miRNAs MiR-103 and MiR-107 to Suppress LRP1 Translation and Promote Cell Death

(A) HCT116 CRISPR Ctrl KO or p53KO cell lines were treated with 10 μM nutlin-3a or vehicle for 24 hr, after which RNA was collected and analyzed for p53-dependent induction of miR-103 and miR-107. Data represent at least two biological replicates, each performed in triplicate. ***$p < 0.001$.

(B) HCT116 cells were treated with the indicated course of Dox for the indicated amount of time, after which RNA was collected and subjected to analysis for miR-103 or miR-107

expression. Data represent at least two biological replicates, each performed in triplicate. *p < 0.05, **p < 0.01.

(C) HCT116 cells were treated with the indicated concentrations of Dox for 24 hr, after which RNA was collected and subjected to analysis for miR-103 or miR-107 expression. Data represent at least two biological replicates, each performed in triplicate. **p < 0.01, ***p < 0.001; NS, non-significant.

(D) U2OS cells were transfected with a luciferase reporter gene to which the WT 3′ UTR of LRP1 or a miR-103/107 mutant was fused. MiR-103 and miR-107 were co-transfected, and the firefly luciferase signal was normalized to constitutively expressed *Renilla* luciferase. Data represent at least two biological replicates, each performed in triplicate. ***p < 0.001; NS, not significant.

(E) HCT116 cells were transfected with the indicated mimics or antagomirs for 24 hr, after which protein lysates were collected and analyzed by western blotting. The relative densitometry values after actin normalization are indicated. Data represent at least two biological replicates.

(F) LRP1 mRNA expression levels were analyzed by RT-PCR after transient knockdown of LRP1 in otherwise unstimulated HCT116 cells using two distinct siLRP1 constructs for the indicated amount of time. Data represent at least two biological replicates, each performed in triplicate.

(G) LRP1 protein expression levels and corresponding cleaved caspase-3 (CC3) levels were analyzed by western blotting in otherwise unstimulated HCT116 cells subjected to transient knockdown for the indicated amount of time. Data represent at least two biological replicates.

(H) Otherwise unstimulated HCT116 cells subjected to transient LRP1 knockdown for 72 hr were stained with propidium iodide and subjected to cell cycle profile analysis by flow cytometry. Data represent at least two biological replicates, each performed in triplicate.

(I) After pretreatment with the indicated antagomirs for 24 hr, HCT116 cells were treated with vehicle or 1 μM Dox for an additional 24 hr. Then cells (including floating cells) were collected and stained with a LIVE/DEAD stain and analyzed by flow cytometry to enumerate the percentage of dead cells. The experiments were performed in triplicate. *p < 0.05.

(J) Model showing that, when subjected to sub-lethal stress, p53 becomes activated and induces the transcription and translation of the target gene *LRP1*. However, when subjected to lethal stress, p53 also induces transcription of the miRNAs miR-103 and miR-107, which feed back and inhibit the translation of *LRP1* mRNA.